Seismological and Geodetic Insights on the North Anatolian Fault Zone through Coda Calibration and InSAR Techniques

Gülşen Tekiroğlu [1,*], Tülay Kaya Eken [1], Kevin Mayeda [2], Jorge Roman-Nieves [2], and Tuna Eken [3]

[1] Boğaziçi University, Kandilli Observatory and Earthquake Research Institute, Department of Geodesy, Istanbul, Türkiye [2]Air Force Technical Applications Center (AFTAC), Florida, USA [3] Istanbul Technical University (ITU), Department of Geophysical Engineering, Istanbul, Türkiye, * present adress: Université Paris Cité, Institut de Physique du Globe de Paris (IPGP), Paris, France

Introduction

The primary motivation of this study is to resolve the inconsistencies in magnitude estimates among regional earthquake catalogs, such as those provided by Kandilli Observatory and Earthquake Research Institute (KOERI) and Disaster and Emergency Management Authority (AFAD). In the existing catalogs, M_w is typically reported for earthquakes with $M_w \geq 4.0$, whereas M_L is used for smaller events. This discrepancy hinders the creation of a homogeneous catalog, which is a fundamental requirement for applications like Probabilistic Seismic Hazard Analysis (PSHA). The map shows the locations of 150 analyzed earthquakes ($3.5 \leq M_L \leq 6.0$) recorded at the seismic stations (triangles) operated by KOERI and AFAD (Fig 1.). A total of 51 earthquakes with $M_L \geq 4$ were analyzed for calibration. The remaining events with $3.5 \leq M_L < 4$ were then estimated based on the calibration results.

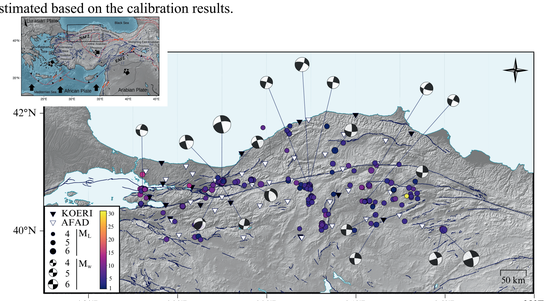

Key contributions of the study

- Validation of earthquake source parameters, homogeneous M_w catalog for small-to-moderate earthquakes
- Signatures of non-self-similar scaling
- Comparing M_w obtained from CCT and InSAR Okada modeling with 2 case studies

Coda Calibration Approach

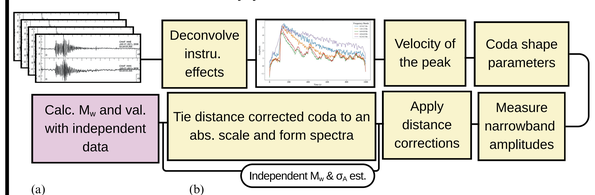

(a)

Evid	192571145
Date	2019-09-14 (257)
Origin time	11:45:59Z
Latitude	40.752
Longitude	32.9668
Depth (km)	10
M_L (model fit)	**4.36 [-0.05, 0.05]**
Apparent stress (model fit)	**0.27 MPa [-0.05, 0.06]**
Energy (model fit)	**10.56 [-0.17, 0.16] log J**
Total energy	10.56 log J
Mc (total energy)	3.84
Observed apparent stress	0.27 MPa
Observed / total energy	77.92 %
Extrapolated / total energy	22.08 %
Validation M_w	4.38
Iterations	28
Data count	262

(b)

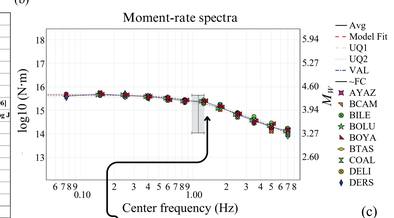

(c)

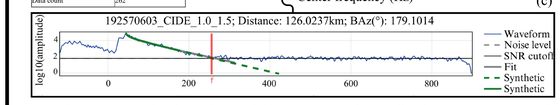

Fig. 2. The spectra results shown in panel (a). The spectra for a validation event (M_w 4.38) showing high consistency with independent magnitude estimates (b). The red dashed line represents the model fit, with the vertical bar indicating the f_c and its 90% confidence interval. A Western US model (blue) is shown for regional comparison. (c) An envelope measurement at 1-1.5 Hz.

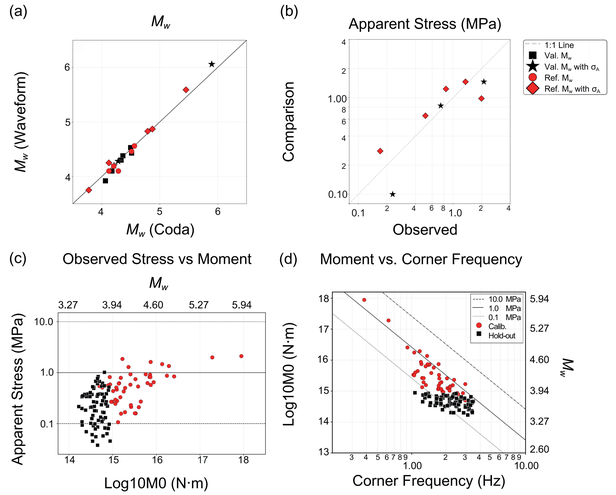

Fig. 3. (a) Coda-derived M_w vs. waveform-modeled M_w (RMS = 0.085). Red symbols denote calibration events; black symbols represent independent validation events. (b) coda-derived σ_A and independent σ_A estimates for both ref. and val. sets. (c) σ_A vs. moment (≥50% measured energy). Calibration (red circles) and hold-out (black squares) events. (d) Obs. f_c vs. M_0 from Brune (1970) spectral fits. Lines indicate constant σ_A of 0.1, 1, and 10 MPa.

Discussion

$$M_0 = \mu A d \quad (1) \quad \text{(Aki, 1966)}$$

$$\sigma_A = \mu \frac{E_R}{M_0} \quad (2) \quad \text{(Wyss, M., \& Brune, J. N., 1968)}$$

$$M_w = \frac{2}{3}(log_{10} M_0 - 9.1) \quad (3) \quad \text{(Hanks \& Kanamori, 1979)}$$

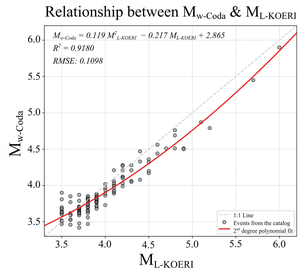

Fig. 7. Comparison between $M_{w\text{-}Coda}$ and $M_{L\text{-}KOERI}$. The 2nd order polynomial fit captures M_L saturation at higher magnitudes, providing a fit compared to the 1:1 line. Analysis included only events where we measured ≥ 65% of the observed total radiated energy.

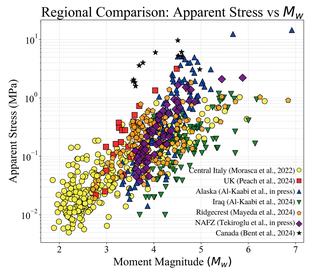

Fig. 8. Comparison of σ_A estimates versus M_w for various tectonic regions. Data points include Central Italy (Morasca et al., 2022), the United Kingdom (Peach et al., 2024), Alaska (Al-Kaabi et al., in press), Iraq (Al-Kaabi et al., 2024), Ridgecrest (Mayeda et al., 2024), Canada (Bent. et al., 2024) and the NAFZ (Tekiroglu et al., in press).

	Strike	Dip	Rake	Slip (m)	$M_{w\text{-}Okada}$	$M_{w\text{-}ref}$	$M_{w\text{-}Coda}$
the 2022 Duzce event	254.490	61.575	-158.0	0.288	6.17	6.06	5.9 ± 0.1
the 2024 Tokat event	176.465	46.00	-28.721	0.155	5.39	5.59	5.45 ± 0.1

Table 1. Preliminary Okada inversion results for the Düzce and Tokat events, comparing of $M_{w\text{-}Okada}$ reference $M_{w\text{-}ref}$ and $M_{w\text{-}Coda}$ estimates.

- σ_A Values range from 0.1 to 2 MPa for M_w 4.0–6.0.
- Non-self-similar scaling.
- Low apparent stress levels indicate a mechanically weak, fluid-rich, and thermally softened crust, consistent with observations in the Sea of Marmara (Chen et al., 2024).

- Utilizing GNSS Troposphere zenith delay to calibrate and remove atmospheric noise from the phase, followed by joint inversions to transform 1D line-of-sight observations into a 3D displacement field for more robust source modeling.

InSAR Coseismic Deformation

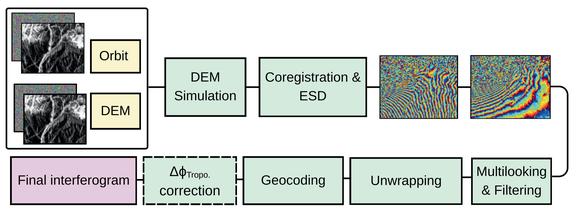

Coseismic LOS displacement maps were generated using a differential InSAR workflow. Topographic phases were removed at full resolution, followed by multilooking and adaptive filtering to maximize SNR. After unwrapping and geocoding, GACOS atmospheric correction and deramping were applied to refine the coseismic signals.

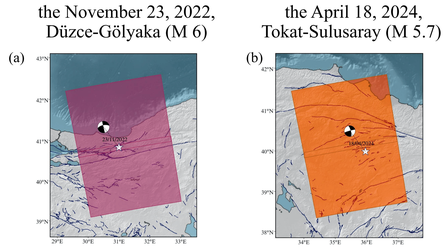

Fig 4. Sentinel-1A ascending frames were used for coseismic deformation analysis of (a) the 2022 Düzce-Gölyaka and (b) the 2024 Tokat-Sulusaray events, with source solutions retrieved from KOERI.White stars show epicenter locations.

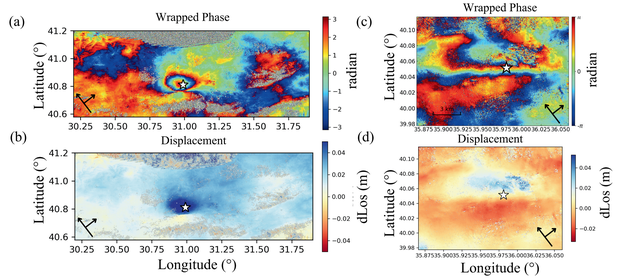

Fig. 5. Coseismic LOS deformation for the (a-b) 2022 Düzce and (c-d) 2024 Tokat events. (a, c) Wrapped interferograms in radians; (b, d) unwrapped displacement in meters.

Okada Inversion & Comparison

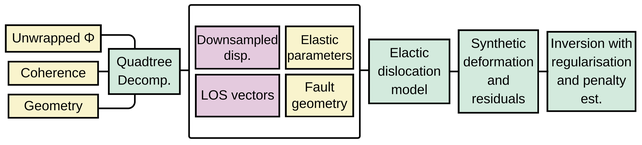

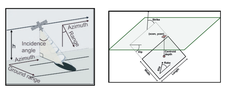

Seismic source modeling workflow. Geodetic data are downsampled via quadtree decomposition to reduce data density while preserving deformation gradients. A geodetic inversion based on the Okada elastic half-space model, constrained by regularization, is performed to estimate the slip distribution. Model reliability is evaluated through the analysis of residuals (penalty).

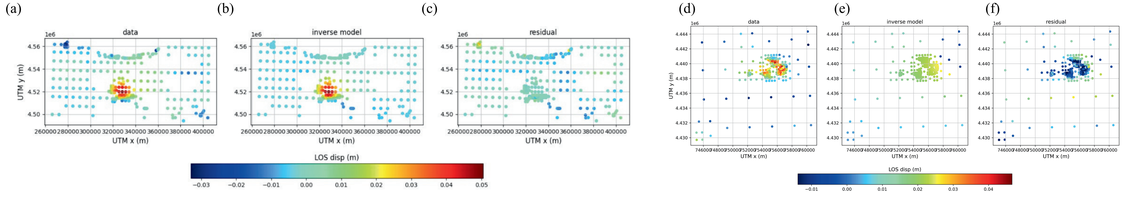

Fig. 6. Source inversion results for the (a–c) 2022 Düzce and (e–f) 2024 Tokat-Sulusaray events. From left to right, panels display downsampled LOS data, best-fit regularized inverse models, and residuals.

Key References

- Al-Kaabi, M., Mayeda, K., Roman-Nieves, J., Chiang, A., Mahdi, H., & Al-Shukri, H. (2024). Using a 1D radially symmetric coda envelope model for robust moment magnitude (M_w) estimation in Iraq's tectonically diverse zones. Bulletin of the Seismological Society of America, 115(3), 1331–1343. https://doi.org/10.1785/0120240113
- Barno, J. (2017). LLNL/Coda-Calibration-Tool [Computer software]. U.S. Department of Energy. https://doi.org/10.11578/dc.20180306.1
- Bianchini, S., Solari, C., & Casagli, N. (2024). A priori estimation of radar satellite interferometry's sensitivity for landslide monitoring in the Italian Emilia-Romagna region. Remote Sensing, 16(13), 2419. https://doi.org/10.3390/rs16132419
- Chen, X., Kwiatek, G., Bindi, D., Becker, D., Bohnhoff, M., Cotton, F., & Martínez-Garzón, P. (2024). Stress drop variations of (a)seismic fault segments in the Sea of Marmara region (northwestern Türkiye) supported by different methodological approaches. Bulletin of the Seismological Society of America, 115(3), 1016–1030. https://doi.org/10.1785/0120240128
- Funning, G. J. (2026). Okapy: A Python tool for Okada elastic half-space modeling [Computer software]. GitHub. https://github.com/geniusinaction/okapy
- Hanks, T. C., & Kanamori, H. (1979). A moment magnitude scale. Journal of Geophysical Research: Solid Earth, 84(B5), 2348–2350. https://doi.org/10.1029/JB084iB05p02348
- Kayrros. (2026). EOS-SAR: A high-performance Python library for SAR and InSAR data processing [Computer software]. GitHub. https://github.com/Kayrros/eos-sar
- Mayeda, K., Hofstetter, A., O'Boyle, J. L., & Walter, W. R. (2003). Stable and reproducible regional magnitudes (M_w) from coda envelopes: Applications to regionalization, locator, and source physics. Journal of Geophysical Research: Solid Earth, 108(B2), 2088. https://doi.org/10.1029/2002JB002175
- Mayeda, K., Roman-Nieves, J., Chiang, A., Gök, R., & Pasyanos, M. E. (2024). Source-scaling comparison and validation for Ridgecrest, California: Radiated energy, apparent stress, and M_w using the Coda Calibration Tool (2.6<M_w<7.1). Bulletin of the Seismological Society of America, 115(3), 890–907. https://doi.org/10.1785/0120240143
- Morasca, P., Bindi, D., Mayeda, K., Roman-Nieves, J., Barno, J., Walter, W. R., & Spallarossa, D. (2022). Source scaling comparison and validation in Central Italy: Data-intensive direct S-waves versus the sparse data coda envelope methodology. Geophysical Journal International, 231(3), 1573–1590. https://doi.org/10.1093/gji/ggac268
- Okada, Y. (1985). Surface deformation due to shear and tensile faults in a half-space. Bulletin of the Seismological Society of America, 75(4), 1135–1154.
- Peach, C., Nippress, S. E. J., Green, D. N., Mayeda, K., Wookey, J. M., & Werner, M. J. (2024). A UK Mw catalogue derived from coda envelopes. Geophysical Journal International, 238(2), 974–991. https://doi.org/10.1093/gji/ggae180
- Tekiroğlu, G., Kaya Eken, T., Mayeda, K., Roman-Nieves, J., & Eken, T. (2026). Source scaling of earthquakes in and around the North Anatolian Fault Zone based on coda-derived source spectra: Toward a more accurate and unbiased Mw catalogue. Geophysical Journal International. (In press)
- Wyss, M. (1970). Stress estimates for South American shallow and deep earthquakes. Journal of Geophysical Research, 75(8), 1529–1544. https://doi.org/10.1029/JB075i008p01529

Contact & Full CV
tekiroglu@ipgp.fr